ELSEVIER

Physica D 81 (1995) 398–410

PHYSICA D

Spatial dynamics of a model for prebiotic evolution

P. Chacón [a,1], J.C. Nuño [b,2,3]

[a] *Dpto. de Bioquímica y Biología Molecular I, Facultad de CC. Químicas, Universidad Complutense de Madrid, 28040 Madrid, Spain*
[b] *Dpto. de Matemáticas, E.T.S.I. de Montes, Universidad Politécnica de Madrid, E-28040 Madrid, Spain*

Received 17 April 1994; revised 12 October 1994; accepted 12 October 1994
Communicated by K. Kaneko

Abstract

The selective properties of a population formed by RNA-like molecules (*replicators*) with catalytic capabilities are analyzed in an extended system. The population evolves in a closed reactor and is kept far from equilibrium by means of a recycling reaction that transforms the degradation products of the replicators into energy rich monomers, from which the species are built up. In the limit of infinite diffusion, for a particular set of parameters the system exhibits tristability between chaos and two fixed points. Under this setup, numerical techniques are used to prove the formation of spatial patterns when finite diffusion forces are taken into account in one- and two-dimensional spaces. Finally, the relevance of these results is discussed within a prebiotic framework.

1. Introduction

The hypothesis that assumes that the first prebiotic material could be mainly formed by RNA-like molecules (here referred to as *replicators*) has obtained wide support after the discovery of the catalytic activity of some RNA molecules (*ribozymes*) [1–3]. These RNA-like molecules with unspecific catalytic capabilities could have formed ensembles of species, the so-called *catalytic networks*.

Although the evolution of these networks has been extensively studied from a theoretical point of view over the last two decades, most of the work has been focused on the analysis of their dynamics under spatially homogeneous conditions [4–7]. Less attention has been paid to the role of diffusion on the behavior of these prebiotic models (see, for instance, Refs. [8–10]). However, it is well known that diffusive forces may play an important role on the dynamics of physical systems (and probably they might occur in the prebiotic soup) [11–13]. Therefore, it ought to be taken into account in mathematical models.

Within the framework of a *RNA-world*, in this paper we attack the problem of pattern formation in one of the theoretical models proposed to study the behavior of catalytic networks [14]. This model is schematically described in Fig. 1. It is a closed system (i.e. only energy can be interchanged with the surroundings) where activated material (nucleotides) react to build up self-replicative units following preestablished rules. These energy rich monomers are regenerated from the by-product of the reaction (obtained mainly as the result of the hydrolysis of the self-replicative species) by means of a recycle mechanism (basically due to an external energy source, e.g. sunlight). The

[1] E-mail: PABLO@solea.quim.ucm.es
[2] E-mail: JUANCA@solea.quim.ucm.es
[3] To whom correspondence should be addressed.

SSDI 0167-2789(94)00214-2

$$I_i + A \xrightarrow{\alpha_i} 2I_i \quad (i)$$
$$I_i + I_j + A \xrightarrow{K_{ji}} 2I_i + I_j \quad (ii)$$
$$I_i \xrightarrow{\delta_i} B \quad (iii)$$
$$B \xrightarrow{\gamma} A \quad (iv)$$

Fig. 1. Kinetic scheme of the model. The meaning of the different reactions is: (i) Each specie I_i, in the presence of the substrate A, selfreplicates noncatalytically with a rate α_i. (ii) The species I_j catalyzes the selfreplication of the species I_i with a rate k_{ij} in the presence of the substrate. (iii) A species I_i degrades in B with a rate δ_i. (iv) The byproduct of the degradation, B, is recyclated in energy high substrate, A, with a rate γ.

closure of the system directly imposes a selection pressure on the population.

The model is described by the following multidimensional partial differential equation:

$$\begin{aligned}
\dot{x}_i(\boldsymbol{r}) &= x_i(\boldsymbol{r})\left[a\left(\alpha_i + \sum_j k_{ji}x_j(\boldsymbol{r})\right) - \delta_i\right] \\
&\quad + \epsilon D_{x_i}\Delta x_i(\boldsymbol{r}) \quad i = 1,\ldots,n, \\
\dot{a}(\boldsymbol{r}) &= \gamma b(\boldsymbol{r}) - \left[a\left(\boldsymbol{r}\right)\left(\sum_i \alpha_i x_i(\boldsymbol{r})\right.\right. \\
&\quad \left.\left. + \sum_i \sum_j k_{ji}x_i(\boldsymbol{r})x_j(\boldsymbol{r})\right)\right] + \epsilon D_a \Delta a(\boldsymbol{r}), \\
\dot{b}(\boldsymbol{r}) &= \sum_i \delta_i x_i(\boldsymbol{r}) - \gamma b(\boldsymbol{r}) + \epsilon D_b \Delta b(\boldsymbol{r}), \qquad (1)
\end{aligned}$$

where x_i, a and b are the concentrations of the self-replicative units, activated and inactivated residues, respectively. The meaning of the kinetic constants are explained in Fig. 1. ϵ may be understood as a dimensionless parameter that scales the reaction-diffusion process. Moreover, it is assumed that the diffusion coefficients are spatial-independent. As usual, $\Delta = \sum_i^{\nu} \partial^2/\partial r_i^2$, ν being the spatial dimension. It is easy to see that system (1) verifies

$$\int_S a(\boldsymbol{r}) + b(\boldsymbol{r}) + \sum_i^n x_i(\boldsymbol{r})\, d\boldsymbol{r} = c, \qquad (2)$$

c being the total concentration of the system. S is the total are of the system.

The local dynamics of this model (obtained after removing the diffusion terms) has already been analysed in a relevant but restricted situation: a system formed by cyclically linked species (a *hypercycle*) [4,14]. Perhaps the most relevant property of this special network is that it allows the coexistence of all the species involved in the organization. Moreover, whereas for networks formed by less than four species the fixed point of coexistence is asymptotically stable, for networks larger than four this fixed point becomes unstable appearing surrounded by a cyclic limit. This fact has special significance when a diffusive process is taken into account (see Ref. [9] and the analysis using cellular automata presented in Refs. [8,10]).

In the next section, we shall show that this dynamic system exhibits chaotic dynamics for a particular set up when diffusive forces are not taken into account. This particular choice will be used as a starting point for the spatial analysis. It is already well known that chaos offers a great variety of behaviors that could be specially reflected when spatial degrees of freedom are considered [15,16]. Section 3 is devoted to demonstrating the formation of spatial inhomogeneities in the extended system under this chaotic local dynamics. Finally, we discuss the possible role that these patterns could have had within the prebiotic scenario.

2. Local dynamics

When, either the system is well stirred (diffusion coefficients tend to infinity) or the diffusion coefficients almost vanish, the spatial behavior of the system is drastically simplified since (1) reduces to a set of ordinary differential equations. Fig. 2 shows the particular model that will be used in the numerical analysis to prove the existence of chaos. The values of the catalytic constants are shown in this figure. In addition, the following set of parameters will be used in all the simulations

$$\begin{aligned}
&\alpha_i = 1, \quad i = 1,2,3,4, \\
&\delta_i = 0.1, \quad i = 1,2,3,4, \\
&\gamma = 1. \qquad (3)
\end{aligned}$$

For this particular setup it can be proven that there are 17 possible fixed points, corresponding to the dif-

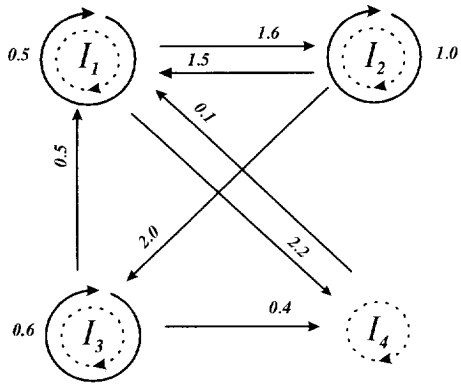

Fig. 2. Schematic plot of the reduced model analysed in the text. The numbers in the arrows represent the particular values of the catalytic constants k_{ij}.

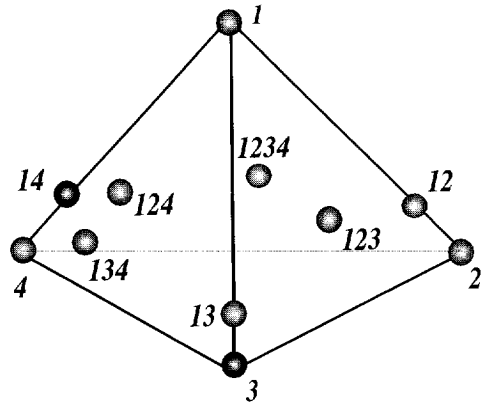

Fig. 3. Schematic location of the steady states for the particular setup described in Fig. 2. Black and grey balls represent stable and unstable fixed points, respectively. The chaotic trajectory surrounds the unstable fixed point {1234}.

ferent coexistence states [6] and the state in which the replicator concentrations is null, i.e. $a = 1$. Apart from them, other attractors of higher dimension may exist, e.g. limit cycles or strange attractors. The existence and the stability properties of these steady states depend on the value of all kinetic constants and in particular on the catalytic constants, k_{ij}. A bifurcation diagram can be made by adding a constant, μ, to the first entry of the catalytic matrix, k_{11}, which will be used as a bifurcation parameter.

The numerical analysis of this model has proven that chaotic dynamics is reached for $\mu = 0$, through a typical Feigembaum cascade (doubling period bifurcations) [17], similar to that shown in Fig. 3 of Ref. [18]. A deeper study demonstrates that the strange attractor is almost contained in a two-dimensional subspace, showing a Lyapunov dimension around 2.05. This chaotic behavior is apparently similar to the strange dynamics reported from the analysis of other related models [18,19]. Again, this coincidence between these results corroborates a statement previously conjectured by Schuster and Sigmund [20]: models based on either the constant organization restriction (CP) or the continuous stirring tank reactor (CSTR) and the recycle model yield to the same behaviour when the concentration of the catalytic species is high enough. In fact, in the latter the system behaves in a subspace characterized by almost constant values of the activated and non-activated monomers, a and b, respectively.

Another aspect that will have special relevance in the analysis of the spatial behavior of the system is the possibility of displaying multistability among different states. In Fig. 3, a global picture for the case $\mu = 0$ is schematically drawn. As can be seen, in addition to the chaotic attractor, there exist two more stable fixed points: one in which all the species vanish except the third, and one that implies the coexistence of species one and four.

3. First evidences of pattern formation

Once the basis of the model has been translated to mathematical symbols, the main purpose of theoreticians is to find analytically the possible solutions of the corresponding expression of (1) for the reduced model and prove their stability properties. Unfortunately, due to the high complexity of the model, as a first approach, only numerical techniques are useful to analyse this reaction-diffusion problem. Essentially, the numerical algorithm reduces the model to a multidimensional coupled map lattice, i.e. a discrete space-time dynamic system [21]. This discret formulation has been extensively used to carry out a deep comparison between the local dynamics and the global spatial behavior [22,23].

To perform this analysis, henceforth we will fix the parameters that define the local dynamics to focus at-

tention on the behavior that is brought about when the diffusion coefficients are varied. The system dynamic is substantially simplified if we consider that all the catalytic species have similar molecular weight and tertiary structure, and therefore, similar diffusion coeficients, i.e. $D_{x_i} = D$ for all $i = 1, 2, 3, 4$. Moreover, we assume that all monomers (activated or not) also have similar values for the diffusion coefficents, $D_a = D_b = d$. These monomers are small subunits that obviously diffuse faster than the larger biopolymers. So that it is assumed that $d \geq D$. Through all the simulations the value of the reaction-diffusion scale factor, ϵ, was arbitrarily chosen to be 10^{-2}. For the spatial coupling, Δ, we take the following scheme:

$$\Delta y(\boldsymbol{r}) = \sum_{j}^{n} y(j) - n y(\boldsymbol{r}), \tag{4}$$

where n is the number of closest neighbors (2 in the 1D-simulations and 4 in the 2D-simulations).

To define completely the problem, both initial and boundary conditions must be specified. Initial conditions are randomly chosen in such a way that the local concentration of the sum of all the species is equal through the whole space, and arbitrarily fixed as 1, i.e.

$$\int_{V} a(\boldsymbol{r}) + b(\boldsymbol{r}) + \sum_{i}^{n} x_i(\boldsymbol{r}) = 1, \tag{5}$$

V being any infinitesimal volume. In the simulations this condition means that the total concentration of all the species is fixed as 1 in each cell. Two physical meaningful boundary conditions are used: *periodic* conditions, that mimic a vast prebiotic scenario in which the effect of the boundary is negligible, and *non-flux* boundary conditions, which would arise in a real scenario when there is no interchange of material with the surroundings (as occurs in this model).

Although the most realistic situation to be considered is a system embedded in a three-dimensional space, there are many cases in which one or two spatial variables can be neglected. That is the case, for instance, when the early biochemical reactions take place within a capillary or on the surfaces of rocks. Therefore, the analysis of the system dynamics in one and two-dimensional spaces can give relevant insights about the actual behavior of this kind of systems.

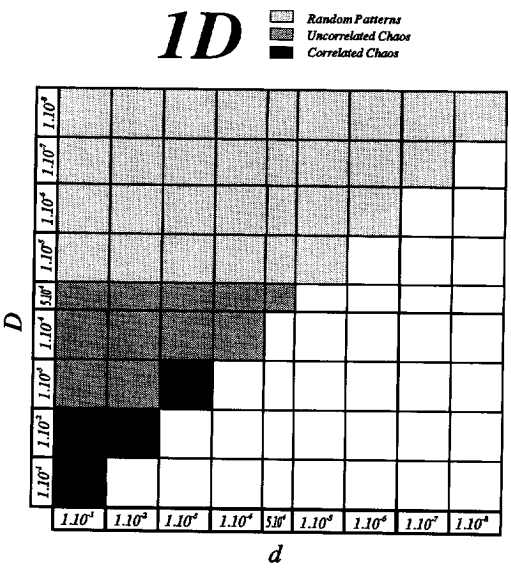

Fig. 4. Schematic representation of D versus d for the 1-dimensional domain. Three regions may be distinguished: homogeneous correlated chaos (black region), the heterogeneous uncorrelated chaos (dark grey region) and a region where random patterns appear (clear grey region).

One-dimensional space

When considering the diffusion coefficients as bifurcation parameters one immediately thinks of the following two obvious limits: on the one hand, at the no-diffusion limit the final state only depends on the initial conditions. There is no way to extract the system from the local attractors. On the other hand, when diffusive forces tend to infinity the system becomes totally mixed, and evolves homogeneously (all the lattice points are in the same state at the same time). Because the strange attractor basin is larger than the attraction basin of the other two fixed points, the final state is likely a spatial coherent chaotic behavior (this fact has been observed in all the simulations).

How does the system behave between these two limits? In Fig. 4, a schematic diagram of the different system behaviors are shown as a function of the ratio between the diffusion coefficients of the replicators, D, and the monomers, d. For $D \geq 10^{-2}$, and indepen-

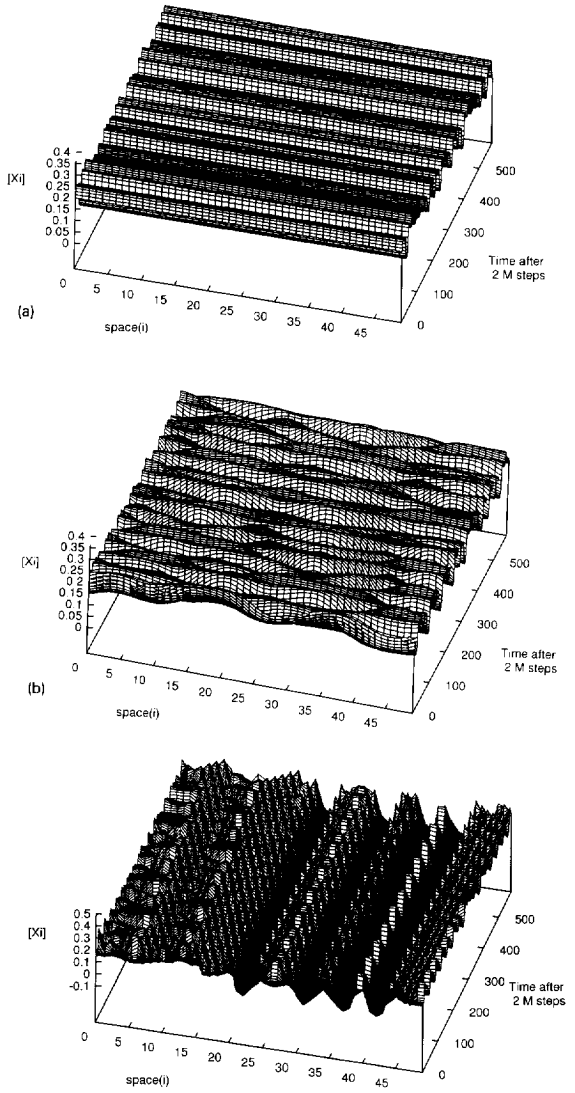

Fig. 5. Temporal evolution of the concentration of I_1 in a 1-D domain with periodic boundary conditions. The diffusion coefficient of the monomers is $d = 10^{-2}$ in all the cases and the diffusion coefficient of the replicators are: (a) $D = 10^{-2}$ (homogenous correlated chaos) (b) $D = 10^{-4}$ (heterogeneous uncorrelated chaos) (c) $D = 10^{-5}$ (random patterns).

dently of d, the system becomes homogeneous, evolving chaotically with time (see Fig. 5a). Each lattice point evolves within the chaotic attractor, totally synchronized with the rest; therefore, the system is in a completely homogeneous phase. The Temporal Power Spectra [TPS] [17] for $D = d = 10^{-2}$ is shown in Fig. 6a. A broad-band spectrum appears, as occurs in the local dynamics, proving the chaotic structure of the system. It is worth to compare this behavior with that obtained from the analysis of a coupled map lattice model with local interactions, where the homogeneous state is unstable. A possible reason for this contradiction is that, in this example, the coherent lenght is of the order of the system size. In fact, as the system lenght increases, this spatially homogeneous and temporally chaotic state disappears in agreement with the coupled map lattice model.

When $10^{-2} > D > 10^{-5}$, and $10^{-1} \geq d > 10^{-5}$, the system still evolves chaotically but now the cells are not in phase (see Fig. 5b). This arrangement does not yet enable the system to develop a coherent spatial patterns. Nevertheless, the main basic modes are already present in the spatial dynamics, as can be clearly seen in the TPS for the case $D = 10^{-4}$, $d = 10^{-2}$ (Fig. 6b): the broad-band typical of chaotic dynamics still remains, although two sharp peaks, corresponding to oscillations of periods two and three, are present. This behavior may be interpreted as just the transition from the previous homogeneous spatial behavior to the formation of spatial patterns. Effectively, as D decreases ($D \leq 10^{-5}$), the diffusive forces are not enough to get the system away from local attractors and therefore, depending on the initial conditions the system brings about a particular stable spatial pattern (see Fig. 5c). As an example, in Fig. 6c, we show the TPS for $D = 10^{-5}$ and $d = 10^{-2}$. These spatial structures remind the frozen random state studied in coupled map lattices [33]. Contrary to the previous cases, now there is an important contribution of frequencies that correspond to high order periods. This fact is a consequence of the coexistence of different attractors such as chaos, chaotic bands and fixed points (which appear perturbed by diffusive forces) (see Fig. 7). The contribution of the chaotic attractors and chaotic bands to the temporal power spectra is evident through the different subharmonics and small broad-band spectrum that still surrounds the sharp peaks (see Fig. 8) [24]. It is interesting to remark that these sharp peaks have been related with strange attractors that have an inner hole (like the Rössler attractor) [25]. However, attractors containing fixed points like that we are dealing with do not have this property and therefore their

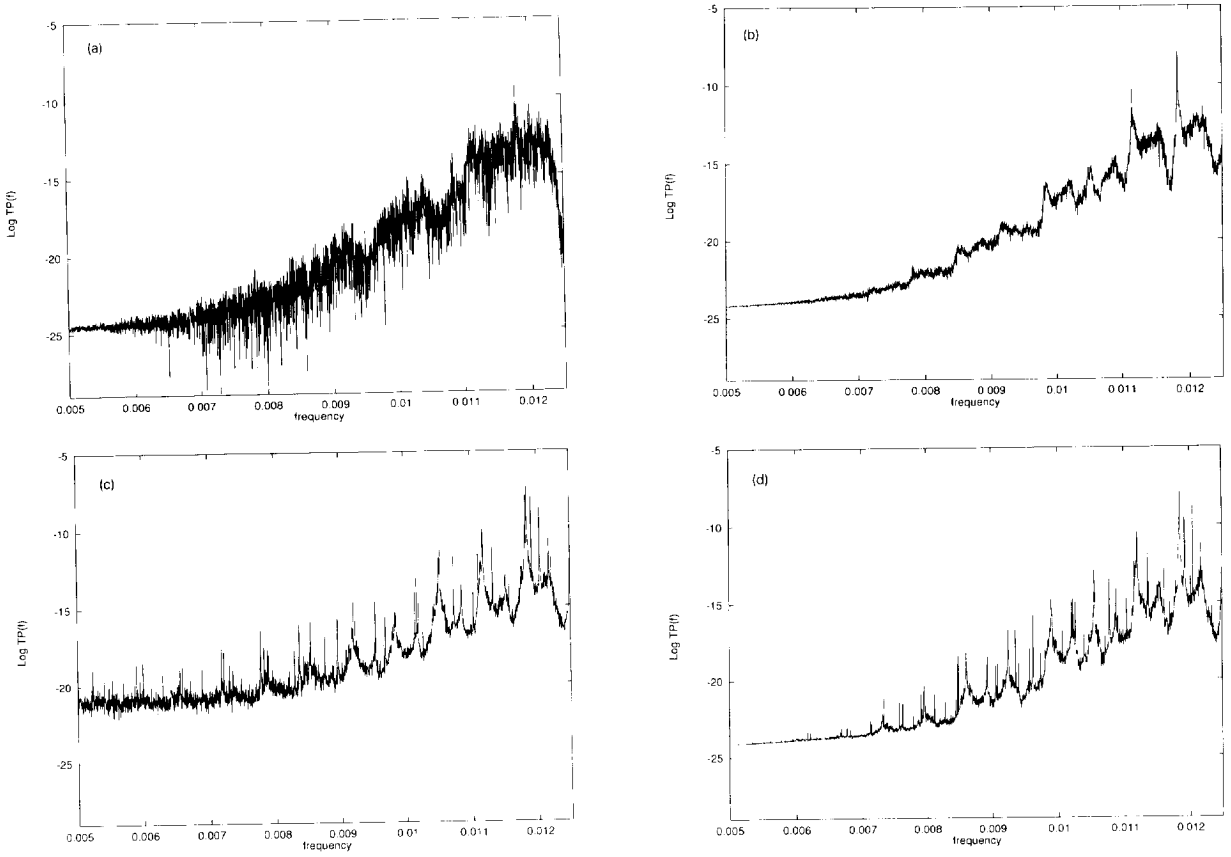

Fig. 6. Figs. 6a, 6b and 6c are the temporal power spectra (TPS) corresponding to the three cases illustrated in Fig. 5, respectively. The TPS in (6d) corresponds to the situation $D = d = 10^{-5}$. The power spectra were obtained from the temporal series of the species I_1 and were calculated using a Fast Fourier Transform (FFT) from 8192 time steps after running out two million transients points, and then averaged from 50 lattice points.

presence in the TPS can only be explained by the formation of different chaotic bands.

These patterns, once formed, remain frozen although locally they evolve governed by the corresponding local attractor. They are characterized by regions that have got a high concentration of the replicators (therefore the energy rich monomers are quickly consumed and there is a high production of energy low monomers), separated by other regions with a low level of replicators (with a higher level of energy rich monomers). Moreover, the size of these aggregates depends on the initial conditions and varies with the ratio between D and d (this fact is well illustrated in Figs. 12a and 12b for the 2-dimensional case).

Another interesting aspect is that this model exhibits spatial patterns even when equal diffusion coefficients are used (compare the TPS drawn in Fig. 6c with that shown in Fig. 6d for $D = d = 10^{-5}$). This fact is not striking since the pattern formation mechanism is strongly correlated with the local dynamics of the system (intrinsically non-linear), unlike the Turing mechanism which has a global character [26].

Two-dimensional space

As in the one-dimensional situation, large values of the diffusion coefficients ($D \geq 10^{-2}$) drive the system to a homogeneous state , in which all the cells evolve chaotically in phase. As long as the diffusion

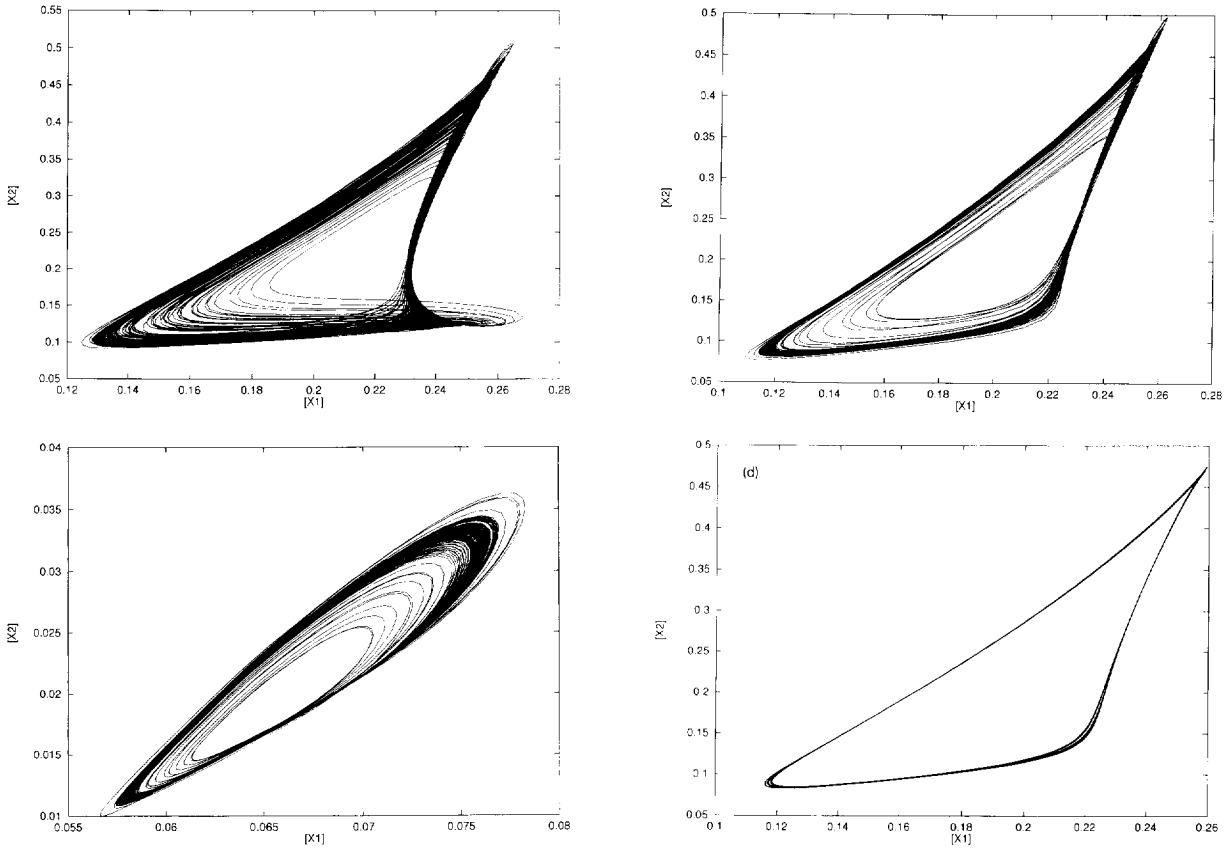

Fig. 7. Consecutive local attractors obtained from the simulation of the system in a 1-dimensional domain (50 lattice points) with $D = d = 10^{-5}$. Each plot represents the concentration of species I_1 versus I_2. (a), (b) and (c) correspond to cells 19, 20 and 21, respectively. Between (c) and (d) (cell 25) there are three cells (not shown) with very low concentration of replicators (even lower than in (c)).

coefficients decrease, the system undergoes a transition to different states, all of them characterized by the formation of complex spatial patterns (see Fig. 10, where several 3D-plots are shown for different choices of the diffusion coefficients).

The different features the system exhibits when evolving in a two-dimensional space are schematically shown in Fig. 9. As may be seen, for approximately $10^{-3} \leq D < 10^{-4}$ and $d \geq 5 \times 10^{-1}$ almost symmetrically distributed aggregates appear (see Fig. 10a). It is interesting to remark the way the system reaches these stationary states. As an example, in Fig. 13 we show a snapshot taken before the system has arrived to the final state. In order to get a stable disposition some of the clusters divide into two separate aggregates. It seems that, for the system to be spatially stable a fixed number of cells evolving almost coherently is needed. As D decreases even more ($D \leq 10^{-4}$) keeping $d \geq 10^{-1}$, a random pattern characterized by a more asymmetric setting of the aggregates appears (Fig. 10b).

As in the 1-dimensional space, the spatial distribution of the aggreagates can be again explained as the result of the interaction among different attractors. The system is organized in such a way that regions with a high concentration of replicators are separated from lower concentration ones, and the boundaries between the clusters remain almost constant in time. However, each aggregate behaves governed by the local dynamics (either chaotic or asymptotically stable). Cluster size increases as d increases and decreases as D decreases as can be seen comparing Figs. 10a and 10b. It

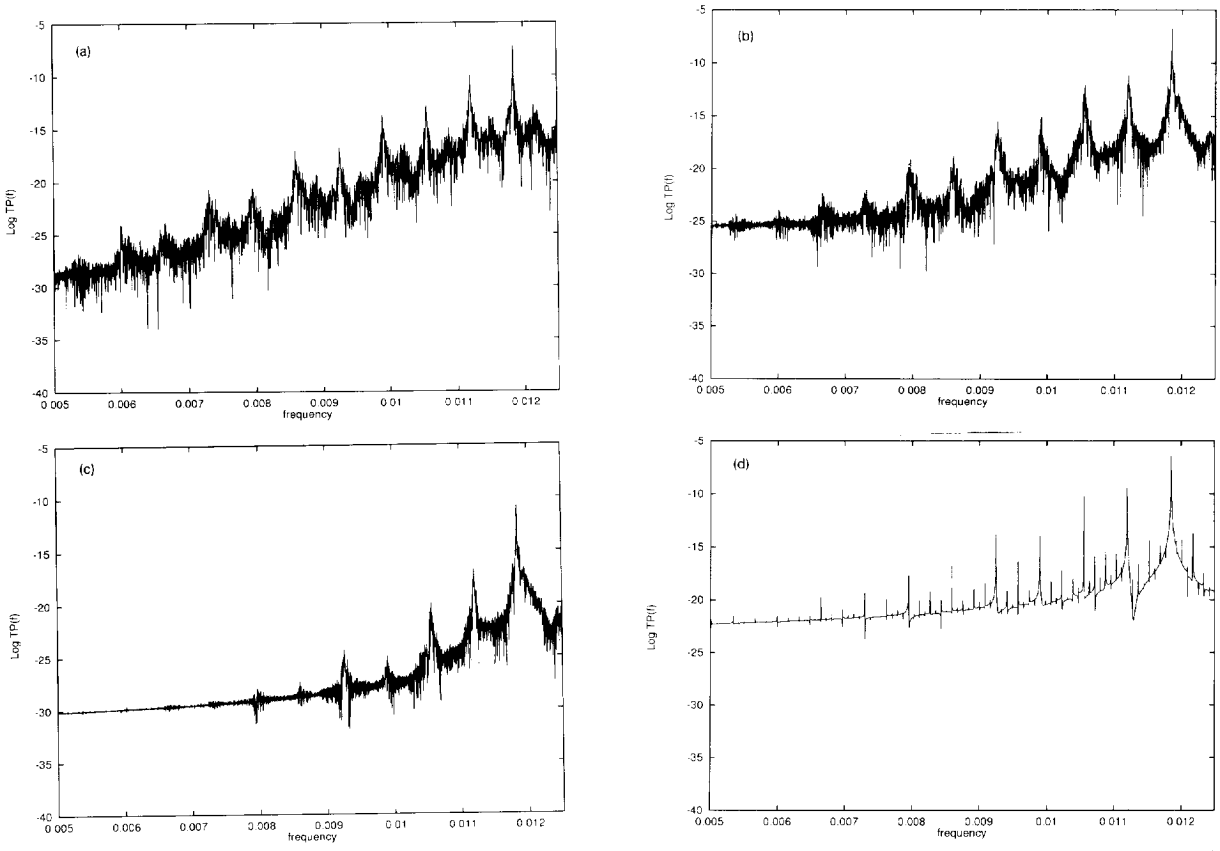

Fig. 8. Corresponding temporal power spectra (without averaging spatially) of the local attractors shown in Fig. 7. As in Fig. 6, these TPS were calculated from the temporal series of I_1 using a FFT from 8192 time steps.

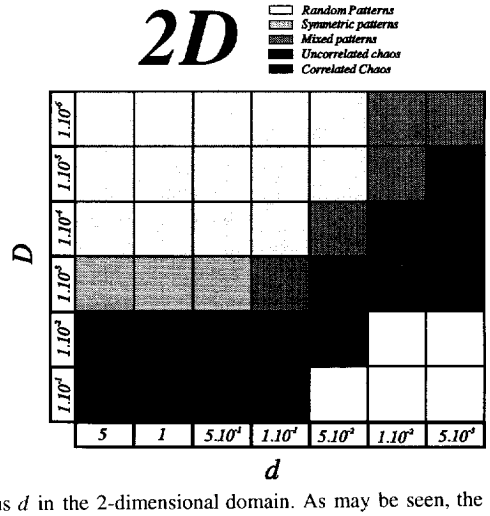

Fig. 9. Schematic diagram of D versus d in the 2-dimensional domain. As may be seen, the behavior of the system is richer than in the 1-dimensional case. In addition to the homogeneous correlated chaos (black region), the heterogeneous uncorrelated chaos (dark grey region) and random patterns (clearest grey region), symmetric and mixed patterns appear as interphases between the other three regions.

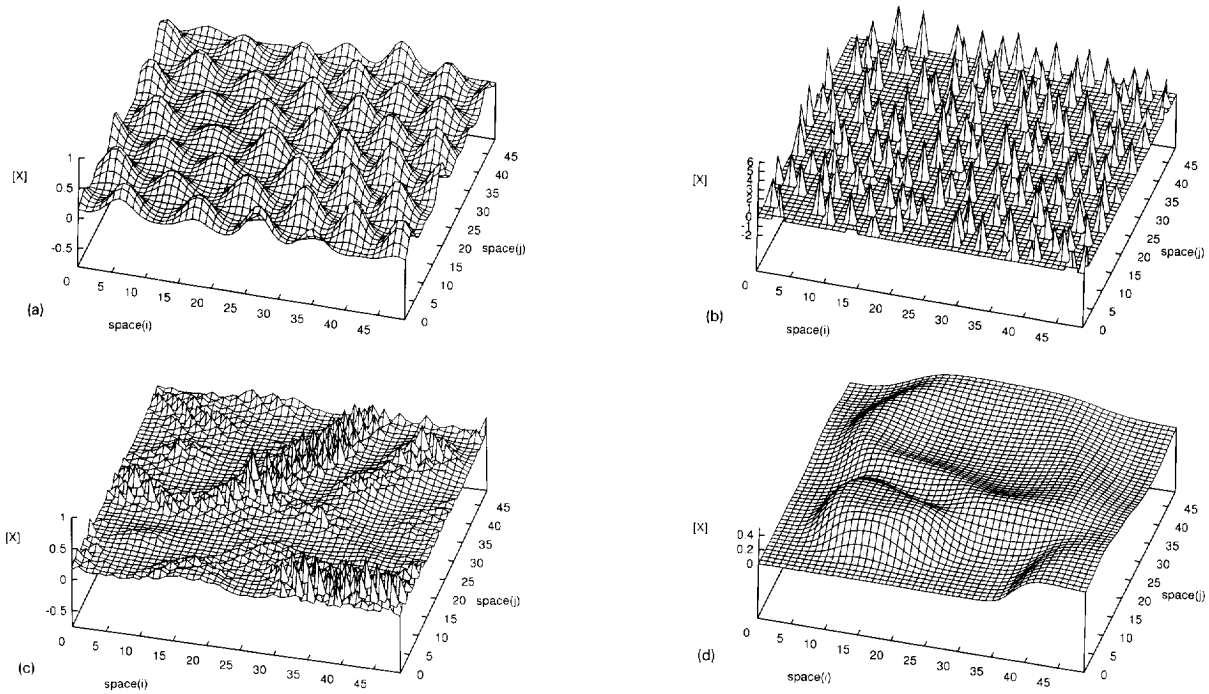

Fig. 10. 3-dimensional plot of the concentration of species I_1 versus space after 2 million steps in a domain with periodic boundary conditions. (a) $D = 10^{-3}$ and $d = 5 \times 10^{-1}$; (b) $D = 10^{-5}$ and $d = 5 \times 10^{-1}$; (c) $D = 10^{-4}$ and $d = 5 \times 10^{-2}$; (d) $D = 10^{-5}$ and $d = 5 \times 10^{-3}$.

turns out that in Fig. 10a all the aggregates are in an almost synchronized state, passing through the maximun level of concentration at the same time (see Fig. 11).

In each cluster, the central cell (of each cluster) is what drives the dynamics of the aggregates with a fully developed chaos. The closest neighbors are influenced by these dynamics and usually exhibit chaotic bands. As we move to the cluster border, chaos dissappears. On the contrary, in Fig. 10b the clusters (most of them formed by only one cell) are totally uncorrelated: cells within a local fixed point basin (and therefore in a quasistationary state) coexist with cells that evolve chaotically.

The symmetric and random patterns dissappear as d decreases giving rise to an incoherent structure in which each cell behaves chaotically but not in phase, as happened in the 1-dimensional case (Fig. 10d). A diffuse interphase (mixed pattern) between this organization and the totally uncorrelated chaotic pattern exist (Fig. 10c). This boundary also separates the random pattern from the totally correlated chaos (homogeneous situation) through $D \approx 10^{-3}$ $d = 10^{-1}$.

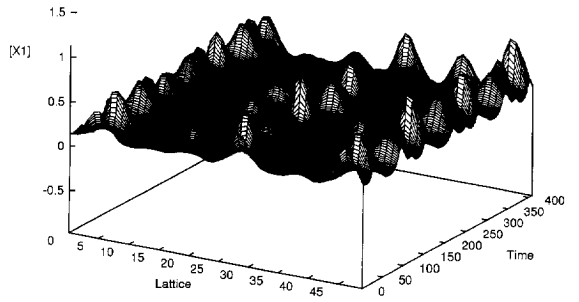

Fig. 11. 3-dimensional plot of the concentration of species I_1 versus space after 2 million steps of row 25 of the 2-dimensional domain with periodic boundary conditions shown in Fig. 10a. As occurs Fig. 5c for the 1-dimensional model, we see clearly that some of the cells are coupled evolving in a complex fashion.

4. Discussion

In this paper we have studied the spatial dynamics of a population formed by selfreplicative species evolving in a closed system by means of a well known

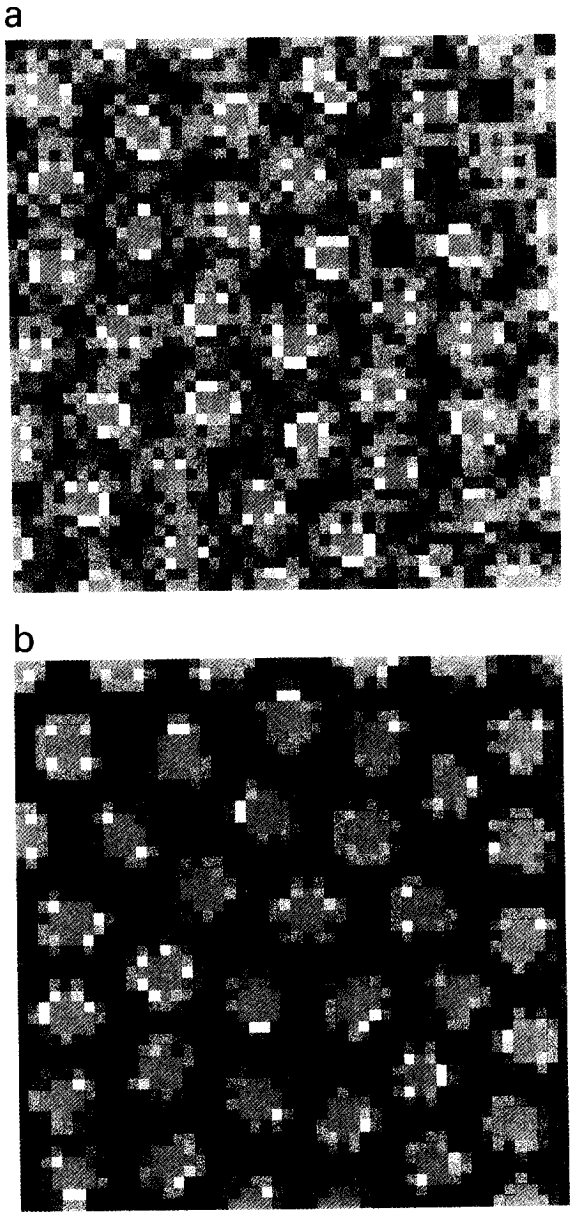

Fig. 12. Snapshots of the total concentration of the replicators at time 2×10^6 in a 2-D domain with non-flux boundary conditions. (a) $D = 10^{-3}$, $d = 5 \times 10^{-1}$; (b) $D = 10^{-3}$, $d = 1$. Red and blue represent the highest and the lowest concentration levels, respectively. Notice the different size of the clusters.

theoretical model [14]. P. Schuster and K. Sigmund [20] conjectured that this model is, under some conditions, equivalent to two other models widely used in molecular evolution when diffusion is not considered:

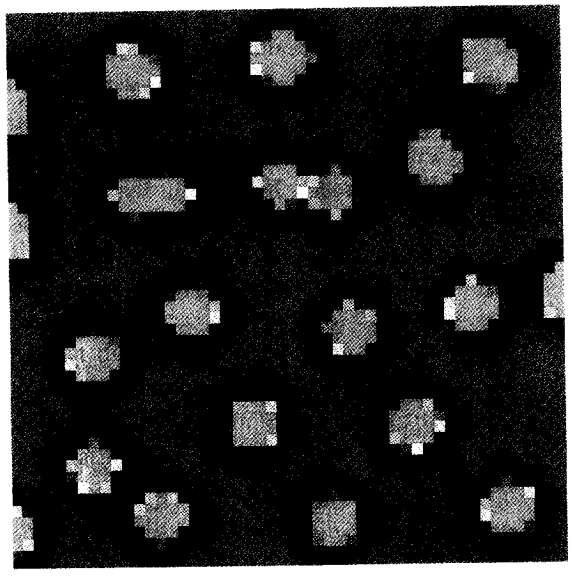

Fig. 13. Snapshot of the total concentration of the replicators at time 1×10^6 in a 2-D domain with non-flux boundary conditions and $D = 10^{-3}$, $d = 5$. As in Fig. 12, red and blue represent the highest and the lowest concentration levels, respectively.

the CSTR (Continuous Stirring Tank Reactor) model and the CP (Constant Population) model. These two models seem to be closer to an experimetal setup but they present a major shortcoming when including diffusion [27]. On the contrary, the model studied here allows a better analysis of the pure diffusive features of the system since no flow of matter with the surroundings exists.

In the homogeneous limit, we have demonstrated the existence of chaotic dynamics for a situation already considered in a previous model under a CP restriction [6,18]. Moreover, the global picture is entirely similar to that already described. Three stable attractors coexist: two fixed points, in which two or three species are not present, and a strange attractor that implies the coexistence of the four species. The concentration of both the rich energy monomers and the byproduct of the degradation reaction remains practically constant.

The same set of parameters that defines these local dynamics was used when diffusion was taken into account. The choice of this setup was guided by two main considerations: firstly, from a theoretical point of view, the coexistence of two stable fixed points

with a chaotic attractor could give rise to an interesting spatial behavior. Secondly, the chaotic dynamics allow the system to interact efficiently with its environment by changing its orbits without changing its coexistence properties, i.e. keeping those species that are structurally necessary. In a certain sense, it could be said that those systems that exhibit a more ordered behavior would not be able to respond adequately to a fluctuating enviroment. Then, by showing an inherent chaotic behavior the system can respond to diffusive forces in a very complicated way, as has been reflected in the great variety of patterns that have been resolved in our simulations.

Numerical integrations were carried out by discretizing both time and space. So, the system has been reduced formally to a multidimensional coupled map lattice. In the bidimensional problem, the space is discretized in such a way that there are only two directions, i.e there is no diagonal diffusion. A scale factor, ϵ, that adequately links the time and spatial dynamics has been introduced. The lattice size was chosen to be small enough to avoid numerical errors but at the same time large enough to reduce the time of the simulations. So, each of the spatial axes was partitioned into 50 cells. Nevertheless, because in some situations large gaps of concentration are created in short distances the integration step might be decreased so low that the real time needed to get a quasistationary state was enormous. To avoid these troubles a more simplified model would be desirable (e.g. a 1-dimensional mapping as suggested by P. Schuster and P.E. Phillipson [28]).

To simplify the analysis we assumed that all the replicators have the same diffusion coefficient, D, as well as the monomers, d. This reduction has allowed us to draw a diffusive phase space as shown in Figs. 4 and 9. It must be remarked that the values of the diffusion coefficients chosen in the simulations are completely arbitrary as well as the rest of the reaction parameters. Thus, a comparison with real diffusion coefficients of biological molecules is not evident.

The study has been carried out in a space of one and two dimensions. As was already pointed out these situations apart from being mathematically relevant, allowing an acceptable numerical analysis, could be used to mimic some interesting biological situations. We have shown the influence of diffusive forces on a set of chaotic attractors that coexist together with different stable fixed points. Whereas for large values of the diffusion coefficients all cells, independently of the initial conditions, are affected by chaotic dynamics (the system gets a coherent phase), as long as diffusion coefficients decrease (the exact dependence on D and d is explained above) diffusion is not able to mix up the initial concentration and its main effect is to cause the splitting of chaotic attractors. This fact brings about a spatial arrangement among different attractors that is ultimately responsible for the formation of the cluster-like pattern observed. However, this mechanism cannot explain the symmetries that appears in the interphase between the correlated chaos state and the random pattern state in the 2-dimensional space.

The stability of these patterns is also interesting. Since no analytical analysis has been done, any stability condition can only be derived from numerical considerations. In this sense, we may say that in all the simulations reported in this work the observed patterns once formed remain after a very long period (about 2 million integration steps). Obviously, that is not proof of stability but it gives an idea of the strength of the spatial organization.

This section would be incomplete without a discussion of the dependence on both the initial conditions and boundary conditions. Concerning the first, all the simulations have been initialized with a random local distribution of the molecular concentration fixed at 1 throughout the system (so that there is not large deviation for a homogeneous global distribution). Moreover, this initial setup allows a straightforward comparison with the dynamics of the system in the limit of no diffusion. Two different kinds of boundary conditions have been used. On the one hand, avoiding wall effects, we have assumed that the system is repeated periodically. On the other hand, non-flux boundary conditions (Neumann conditions) enable us to study the influence of the surroundings barriers on the system behavior. No measurable differences have been noticed, i.e. the situations described above appear independently of the boundary conditions used. How-

ever, a more detailed study would probably detect relevant differences on the dynamics.

The behaviour depends strongly on the network architecture. In previous papers, it has been demonstrated that a population of replicators formed by species cyclically linked (a hypercycle) evolving either under a CP restriction [8] or on a recycle system [9,10] gives rise to spiral patterns where one or more spirals coexist in the system. Following these authors, these models show very good stability properties, and they do not allow the formation of aggregates of the kind described in this work. Nevertheless, these results have been questioned recently by Cronhjort and Blomberg by analysing a two-dimensional partial differential equations model [32]. Undoubtedly, this contradictory conclusions should be solved in order to get a right understanding of the theoretical relationship between reaction-diffusion models based on partial differential equations and those based on cellular automata.

Since M. Eigen (and lately together with P. Schuster) [29, 4] formulated the selection and evolution of simple selfreplicative units in mathematical terms a new way of thinking about prebiotic evolution came about. After more than two decades developing the proposed models a wide variety of mathematical conclusions have been proved. Among them and, maybe because it is now based on well demonstrated empirical results [30], there is one that deserves a special mention here: two or more selfreplicative species can take advantage of a their catalytic capabilities and coexist to create a new order in a higher level of organization.

These results strengthen the hypothesis of a prebiotic scenario where all the metabolic necessities were carried out by RNA-like molecules. The major shortcoming of this hypothesis appears when one is tempted to explain the origin of cellular structures from it. And indeed, present life forms are cellular everywhere, i.e. the genetic material is encapsulated and, therefore isolated from the surroundings. Would it be possible to explain the origin of a precellular scenario from these RNA-like based models? At present many details are unknown and it is difficult to suggest a plausible way to go ahead at this stage of prebiotic evolution.

However, we think that this contribution might give some insight in this direction. Throughout this paper we have studied a model that mimics the evolution of selfreplicative species in a heterogeneous medium. As has been stated in Section 3, for particular choices of the diffusion coefficients a process of self-organization takes place driving the system to a state in which high population density regions are separated by low concentration ones. These low populated areas act as real barriers to the transport of information carriers. Roughly speaking, it could be said that the system has undergone a spatial compartimentation. As has been repeatedly stated [13,31] compartimentation must appreciably change the selective and evolutive features of the system. This matter will be the subject of a forthcoming paper.

Acknowledgements

We greatly appreciate the helpful discussions with our colleagues of the Biophysics group from the Department of Biochemistry and Molecular Biology at the *Universidad Complutense* of Madrid. We would like to recall that the basic ideas behind this work were born in Vienna, during the stay of one of the authors (JCN) at the *Institut für Theoretische Chemie* in 1992. This work was partially supported by grants from DGICYT (Spain) projects PB91-222 and PB92-0908. We also thank Prof. Christopher Dove for correcting the English style.

References

[1] T.R. Cech and B.L. Bass, Ann. Rev. Biochem. 55 (1986) 599.
[2] J.A Doudna and J.W Szostak Nature 339 (1989) 519.
[3] G.F. Joyce, Nature 338 (1989) 217.
[4] M. Eigen and P. Schuster, The Hypercycle – A Principle of Natural Self-Organization (Springer, Berlin, 1979).
[5] J. Hofbauer and K. Sigmund, The Theory of Evolution and Dynamical Systems (Cambridge Univ. Press, Cambridge, 1988).
[6] J.C Nuño, M.A. Andrade, F. Morán and F. Montero, Bull. Math. Biol. 55 (1993) 385.
[7] J.C Nuño, M.A. Andrade and F. Montero, Bull. Math. Biol. 55 (1993) 417.
[8] M.C. Boerlijst and P. Hogeweg, Physica D 48 (1991) 17.

[9] C. Streissler, Autocatalytic Networks Under Diffusion, Doctoral thesis (Universität Wien, Wien, 1992).
[10] P. Chacón, J.C. Nuño and F. Morán, An. Quim. 6 (1993) 379.
[11] M.C. Cross and P.C. Hohenberg, Rev. Mod. Phys. 65 (1993) 851.
[12] J.D. Murray, Mathematical Biology (Springer, Berlin, 1990).
[13] P. Schuster and K. Sigmund, From Biological Macromolecules to protocells - The principle of early evolution, in: Biophysics, eds. W. Hoppe, W. Lohmann, H. Markl and H. Ziegler, (Springer, Berlin, 1982).
[14] J. Hofbauer and P. Schuster, Dynamics of Linear and Nonlinear Autocatalysis and Competition in Stochastic Phenomena and Chaotic Behavior in Complex Systems (Springer, Berlin, 1984).
[15] K. Kaneko, Physica D 37 (1989) 60.
[16] A.S. Mikhailov and A.Y. Loskutov, Foundations of Synergetics II - Complex Patterns (Springer, Berlin, 1991).
[17] M.J. Feigembaum, J. Stat. Phys. 19 (1978) 25.
[18] M.A. Andrade, J.C. Nuño, F. Morán, F. Montero and G.J. Mpitsos, Physica D 63 (1993) 21.
[19] W. Schnabl, P.F. Stadler, C. Forst and P. Schuster, Physica D 48 (1991) 65.
[20] P. Schuster and K. Sigmund, Ber. Bunsenges. Phys. Chem. 89 (1985) 668.
[21] K. Kaneko, Prog. Theor. Phys. 72 (1984) 480.
[22] R.V. Solé, J. Valls and J. Bascompte, Phys. Lett. A 166 (1992) 123.
[23] S. Sinha, D. Biswas, M. Azam and S.V. Lawande, Phys. Rev. A 46 (1992) 6242.
[24] B. Hao and S. Zhang, J. Stat. Phys. 28 (1982) 769.
[25] J. Crutchfield, D. Farmer, N. Packard, R. Shaw, G. Jones and R.J. Donnelly, Phys. Lett. A 76 (1980) 1.
[26] A.M. Turing, Philos. Trans. R. Soc London Ser. B 237 (1952) 37.
[27] E.D. Weinberger, Bull. Math. Biol. 53 (1991) 623.
[28] P.E. Phillipson and P. Schuster, unpublished.
[29] M. Eigen, Naturwissenschaften 58 (1971) 465.
[30] M. Eigen, C.K. Biebricher and M. Gebinoga, Biochemistry 30 (1991) 11005.
[31] M. Eigen and R. Winkler-Oswatitsch, Steps Towards Life: A Perspective on Evolution (Oxford Univ. Press, Oxford, 1992).
[32] M.B. Cronhjort and C. Blomberg, J. Theor. Biol 169 (1994) 31.
[33] K. Kaneko, Physica D 34 (1989) 1.